

## FTIR AND XRD INVESTIGATIONS OF TETRACYCLINE INTERCALATION IN SMECTITES

ZHAOHUI LI<sup>1,3,4,\*</sup>, VERA M. KOLB<sup>2</sup>, WEI-TEH JIANG<sup>3</sup>, AND HANLIE HONG<sup>4</sup>

<sup>1</sup> Geosciences Department, University of Wisconsin – Parkside, Kenosha, WI 53141-2000, USA

<sup>2</sup> Chemistry Department, University of Wisconsin – Parkside, Kenosha, WI 53141-2000, USA

<sup>3</sup> Department of Earth Sciences, National Cheng Kung University, 1 University Road, Tainan 70101, Taiwan

<sup>4</sup> Faculty of Earth Sciences, China University of Geosciences, Wuhan, Hubei, 430074, China

**Abstract**—Due to swelling, smectite minerals are capable of intercalating many organic molecules in their interlayer space. Tetracycline (TC) is a group of antibiotics used extensively in human and veterinary medicine. The great aqueous solubility and long environmental half life of TC mean that the study of interactions between swelling clay minerals and TC are of great importance in TC transport and retention in subsurface soils. In the present study, the intercalation of TC molecules at different levels into smectites was investigated using Fourier transform infrared spectroscopy (FTIR) and X-ray diffraction (XRD). The shift of the FTIR bands of amide I and II in comparison to crystalline TC suggested a strong interaction between the amide groups and the clay surfaces. The band at  $1455\text{ cm}^{-1}$  remained the same after TC intercalation into SAz-1, SWy-2, and SYn-1, suggesting that complexation was not a dominant mechanism of TC uptake by these minerals. With cation exchange as the major mechanism of TC intercalation into these minerals, simultaneous removal of  $\text{H}^+$  from solution protonated the TC molecules and provided a positive charge to interact with negatively charged mineral surfaces even in neutral to slightly alkaline conditions. The increase in interlayer distance after intercalation by TC, as revealed by XRD, suggested a tilted orientation of the intercalated TC molecules in both twisted conformation in acidic condition and extended conformation in alkaline condition.

**Key Words**—Cation Exchange, Complexation, Deuterated Tetracycline, pH, Swelling Clay, Surface Adsorption.

### INTRODUCTION

Antibiotics are used extensively in human and veterinary medicine, as well as in aquaculture for the purpose of preventing (prophylaxis) or treating microbial infections (Kümmerer, 2009). In 2000,  $>22.7 \times 10^7$  kg of antibiotics were produced in the United States and  $>40\%$  of them were used as feed supplements to enhance animal growth (Wang *et al.*, 2008). The extensive use of pharmaceuticals results in their frequent detection in final effluents after treatments from wastewater treatment plants in Canada (Miao *et al.*, 2004), Europe (Carballa *et al.*, 2004), the United States (Batt and Aga, 2005), and Australia (Al-Rifai *et al.*, 2007).

At present, conventional wastewater-treatment plants are not designed or operated to remove very low concentrations of contaminants, including pharmaceuticals and personal-care products, which may cause the release of these compounds into surface waters (Kolpin *et al.*, 2002). A recent survey in 1999–2000 of 139 US streams detected 82 out of the 95 organic wastewater

contaminants monitored, with many of them being antibiotics and growth hormones (Kolpin *et al.*, 2002).

Tetracycline (TC) is a group of compounds that are amphoteric due to the presence of both Lewis base and Lewis acid functional groups (Sarmah *et al.*, 2006). The notation of charge on different functional groups is indicated by a 3-character sequence using +, –, and 0 to represent positive, neutral, and negative charges with the first position representing the dimethylammonium (C4) group, the second position the phenolic diketone moiety (C10–C12), and the third position the tricarbonyl system (C1–C3) (Figure 1). TC is present as (1) a cation, +00, below pH 3.3, due to the protonation of the dimethylammonium group; (2) as a zwitterion, +–0, between pH 3.3 and 7.7, due to the loss of a proton from the phenolic diketone moiety; (3) as a monovalent anion, +––, between pH 7.7 and 9.7, from the loss of another proton from the tricarbonyl system; and (4) as a divalent anion, 0––, above pH 9.7, due to deprotonation from the dimethylammonium group (Kulshrestha *et al.*, 2004). The values of sorption coefficients,  $K_d$ , for cations +00 on soils or clays were more than an order of magnitude larger than those of zwitterions +–0 and anions +–– (Wang *et al.*, 2008).

Tetracycline is extremely persistent in the environment over time. For example, the 50% and 90% dissipation rates (DT50 and DT90) of oxytetracycline

\* E-mail address of corresponding author:

li@uwp.edu

DOI: 10.1346/CCMN.2010.0580402

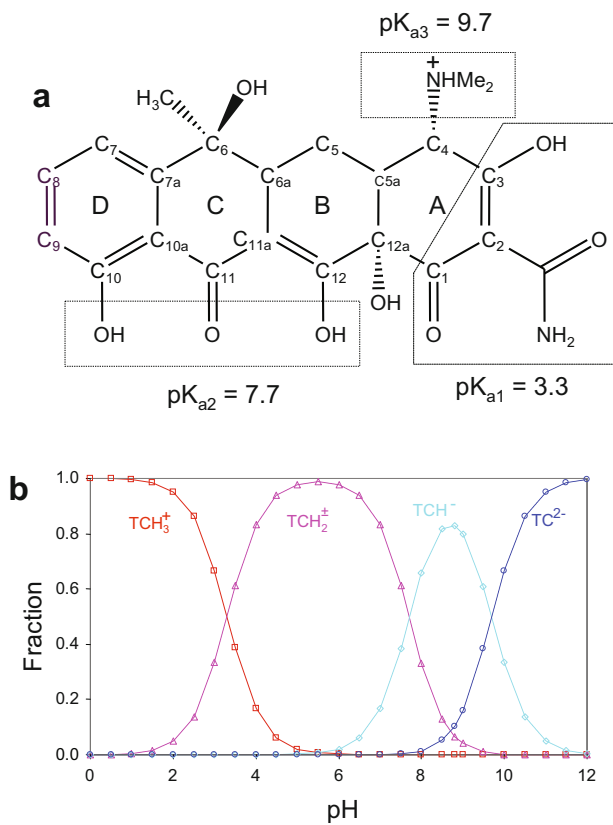


Figure 1. (a) Plan view of the molecular structure of TC, and (b) speciation of TC at different pH values.

(OTC) were 21.7 and 98.3 days under surface run-off field conditions when liquid pig manure fortified with OTC was applied to sandy loam soil plots (Blackwell *et al.*, 2007). The principal mechanism of TC removal from activated sludge was by sorption, with no evidence of TC biodegradation being observed during a biodegradability test using a sequence batch reactor (Kim *et al.*, 2005).

The sorbents tested to remove TC included montmorillonite (Porubcan *et al.*, 1978; Kulshrestha *et al.*, 2004; Figueroa *et al.*, 2004; Parolo *et al.*, 2008; Li *et al.*, 2010), soils (Sassman and Lee, 2005), iron oxides (Figueroa and Mackay, 2005; Gu and Karthikeyan, 2005), humic materials (Gu *et al.*, 2007), silica (Turku *et al.*, 2007), palygorskite (Chang *et al.*, 2009a), and rectorite (Chang *et al.*, 2009b). Most of the studies were focused on the pH effect on TC sorption. Only limited investigations have been conducted to elucidate the state of adsorbed TC molecules in the interlayer space of swelling clay minerals. In the present study, FTIR and XRD analyses were performed to study the interaction between TC molecules and the smectites in order to decipher the configurations of intercalated TC molecules in the interlayer space of smectites at different TC intercalation levels.

## MATERIALS AND METHODS

### Materials

The smectites used were SWy-2, a Na<sup>+</sup>-montmorillonite; SAz-1, a Ca<sup>2+</sup>-montmorillonite; SYn-1, a synthetic mica-montmorillonite containing NH<sub>4</sub><sup>+</sup> in the interlayer (Madejová and Komadel, 2001); and SHCa-1, a hectorite (a Li<sup>+</sup>-bearing trioctahedral smectite). They were obtained from the Source Clays Repository of The Clay Minerals Society and were used without further purification. The cation exchange capacities (CEC) are 85±3, 123±3, 70–140, and 66±4 meq/100 g, respectively (Borden and Giese, 2001). The layer charges are 0.32, 0.35, 0.24, and 0.23 eq per half unit cell, i.e. (Si,Al)<sub>4</sub>O<sub>10</sub>, respectively (Mermut and Lagaly, 2001). The external surface areas are 23, 65, 118, and 36 m<sup>2</sup>/g, respectively (Dogan *et al.*, 2006).

Tetracycline hydrochloride was purchased from Calbiochem (Darmstadt, Germany). It has a formula weight of 480.9 g/mol and pK<sub>a1</sub>, pK<sub>a2</sub>, and pK<sub>a3</sub> values of 3.3, 7.7, and 9.7, respectively (Kulshrestha *et al.*, 2004).

### Tetracycline intercalation

To each 50 mL centrifuge tube 0.10 g of smectite and 20 mL of TC solution at concentrations of

100–3000 mg/L were added and mixed on a reciprocal shaker at 150 rpm for 24 h at room temperature. During mixing, the centrifuge tubes were wrapped in aluminum foil to prevent light-induced decomposition. The solution pH was not adjusted in order to minimize the influence of cations from added salt on TC adsorption and intercalation. The initial solution pH was determined by the input concentration of HCl associated with TC while the equilibrium solution pH was measured. After mixing, samples were centrifuged at 7600 rpm for 20 min and the supernatant analyzed for equilibrium TC concentrations by an HPLC method (see below). The amount of TC adsorbed was determined by the difference between initial and equilibrium concentrations. The removal of  $H^+$  from solution was determined from the difference between the initial and equilibrium solution pH. All experiments were run in duplicate. After removal of the supernatant, the solid samples were re-suspended in distilled water and the suspensions were

deposited on glass slides to make oriented samples for XRD analysis. Portions of the powder samples after XRD analyses were used for FTIR analysis.

#### Method of deuteration

Deuteration was achieved following the same liquid to solid ratio with the liquid being  $D_2O$ . Mixtures were heated at  $65^\circ C$  for 1 week with a Hybaid Micro-4 (Middlesex, UK) instrument at a rotation rate of 6 rpm. The mixture was then transferred to a desiccator and vacuum dried before an FTIR measurement was taken.

#### Methods of analyses

The aqueous TC concentration was determined by an HPLC method (Chang *et al.*, 2009a, 2009b) using a GBC 1202 pump (Hampshire, Illinois, USA), an Asahipak ODP-504E column (Shodex, Showa Denko, Japan), and a GBC LC1205 UV-Vis detector at 254 nm. The mobile phase was 0.01 M phosphoric acid/acetonitrile (75:25)

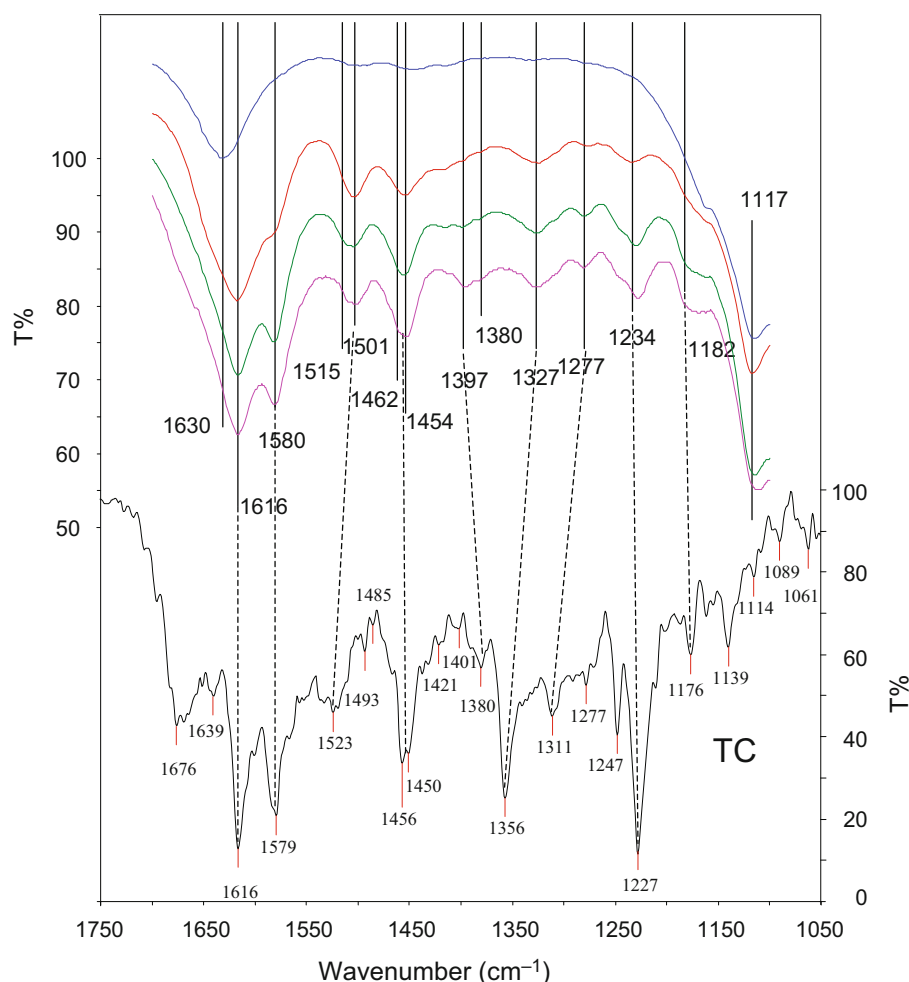


Figure 2. FTIR spectra of SWy-2 intercalated with 0.25, 0.50, 0.84, and 0.91 CEC of TC at equilibrium solution pH values of 7, 6, 4, and 3.5 (top to bottom).

with the pH adjusted to 2.5. At a flow rate of 1.5 mL/min, the retention time was 6 min. A linear calibration was made with five standards between 5 and 100 mg/L with an  $r^2$  of no less than 0.99. The amount of TC adsorbed was normalized to the CEC of each mineral.

The FTIR spectra of the air-dried samples were acquired on a Perkin Elmer Spectra One Spectrometer equipped with a diamond-press Attenuated Total Reflection accessory. The spectra were obtained from 450 to 4000  $\text{cm}^{-1}$  by accumulating 256 scans at a resolution of 4  $\text{cm}^{-1}$ .

Powder XRD analysis was performed on a Rigaku D/Max-IIIa diffractometer with Ni-filtered  $\text{CuK}\alpha$  radiation at 30 kV and 20 mA. Randomly oriented samples were made for pure TC solid and data were collected from 2 to 70°2 $\theta$ , while oriented specimens prepared for TC-intercalated smectites were analyzed from 2 to 20°2 $\theta$ . The scanning rate in each case was 2°/min with 0.01° per step. A 1° divergent slit, 1° scatter slit, and 0.3 mm receiving slit were used.

## RESULTS AND DISCUSSION

### *FTIR spectra of smectites intercalated with different amounts of TC*

The full FTIR spectra of smectites intercalated with different amounts of TC were not plotted as the band positions corresponding to the smectites are almost identical to the published data for standard clays (Madejová and Komadel, 2001). Only the 1050–1750  $\text{cm}^{-1}$  band range was plotted, therefore, to illustrate the characteristic TC bands (Figures 2–5). The consistency in band positions suggests that TC intercalation in smectites caused no major changes in bonding strength to the phyllosilicate backbone. The only noticeable difference was a systematic decrease in band position corresponding to the OH deformation of water at 1630  $\text{cm}^{-1}$ , as the amount of TC adsorbed increased, which could be attributed to the influence of C=O vibration in ring A or a gradual decrease of interlayer water content with an increase in TC adsorption (Figure 3).

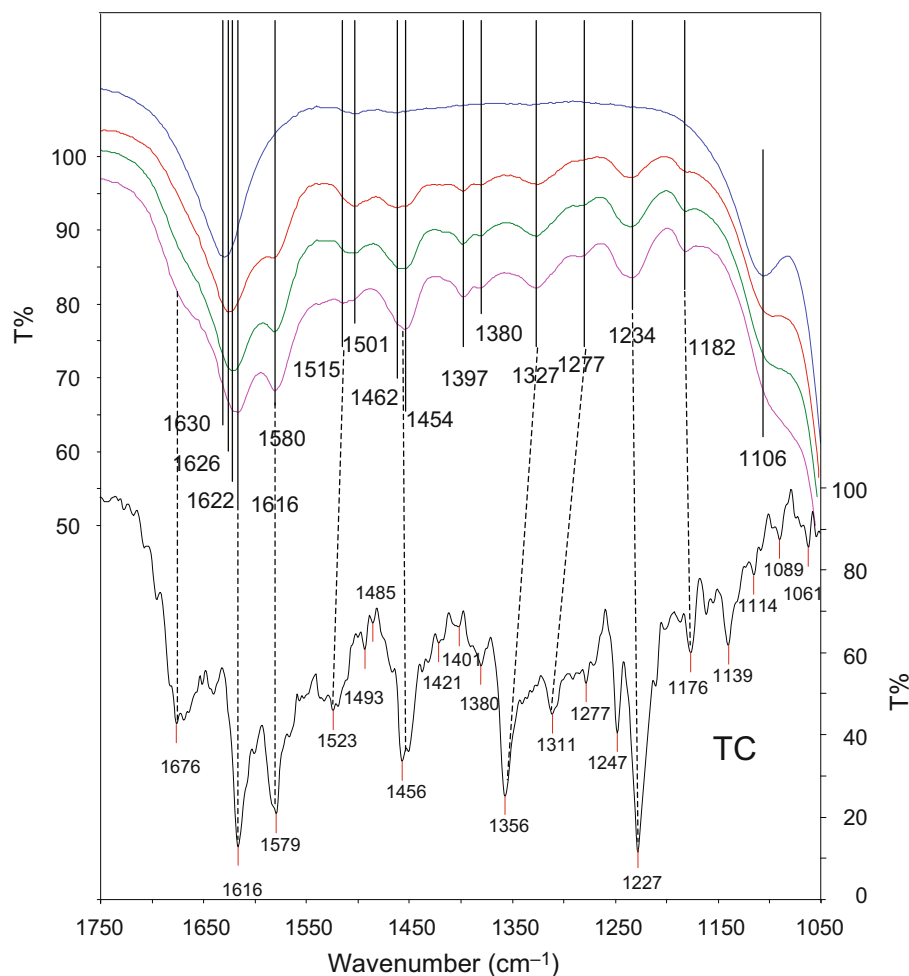


Figure 3. FTIR spectra of SAZ-1 intercalated with 0.18, 0.34, 0.63, and 0.77 CEC of TC at equilibrium solution pH values of 5, 4, 3.8, and 3.4 (top to bottom).

Table 1. FTIR band positions (cm<sup>-1</sup>) for crystalline TC and TC intercalated into SAz-1 and SWy-2 at different intercalation levels.

TC acid <sup>§</sup>	TC base <sup>§</sup>	Crystal-line TC <sup>‡</sup>	SAz-1				SWy-2				Possible band assignment <sup>†</sup>
			Amount of TC intercalated as a fraction of CEC								
			0.18	0.34	0.63	0.77	0.25	0.50	0.84	0.91	
1669	1650	1676									C=O amide or Amide I <sup>¶</sup>
1618		1616		1626	1622	1616		1618	1617	1617	C=O A ring
1582	1585	1579		1580	1580	1580		1582	1583	1581	C=O C ring
1520	1513	1523	1502	1503	1506	1513	1496	1504	1503	1502	NH <sub>2</sub> amide or Amide II <sup>¶</sup>
1450	1462–1448 1402–1390	1456	1462	1462	1454	1455	1445	1453	1456	1453	C=C skeleton
				1398	1390	1397	1411	1417	1414		
1375		1380		1380	1380	1380			1398	1397	
1356	1354	1356									
1311	1311	1311	1333	1325	1326	1327	1329	1324	1326	1326	
1280	1275	1277			1282	1282		1277	1281	1282	
1248	1248	1247									
1228	1225	1227	1235	1235	1236	1234		1235	1230	1228	C-N amide or Amide III
1175	1173	1176		1182	1181	1181			1161	1170	
1139	1125	1139									
1111		1114									
1060	1065	1061									

<sup>§</sup> peaks from Schlecht *et al.* (1974)

<sup>†</sup> from Gu and Karthikeyan (2005)

<sup>‡</sup> from the present study

<sup>¶</sup> from Caminati *et al.* (2002)

Table 2. FTIR band positions (cm<sup>-1</sup>) for crystalline TC and TC intercalated into SYn-1 and SHCa-1 at different intercalation levels.

TC acid <sup>§</sup>	TC base <sup>§</sup>	Crystal-line TC <sup>‡</sup>	SHCa-1				SYn-1				Possible band assignment <sup>†</sup>
			Amount of TC intercalated as a fraction of CEC								
			0.34	0.68	1.20	1.23	0.29	0.48	0.50	0.52	
1669	1650	1676									C=O amide or Amide I <sup>¶</sup>
1618		1616	1615	1617	1614		1618	1617	1617	1615	C=O A ring
1582	1585	1579		1598	1596	1595	1579	1579	1579	1579	C=O C ring
1520	1513	1523		1497	1494	1495	1499	1500	1492	1499	NH <sub>2</sub> amide or Amide II <sup>¶</sup>
1450	1462–1448 1402–1390	1456	1436	1439	1435	1436	1448	1452	1452	1452	C=C skeleton
			1407	1411	1408	1408				1401	
1375		1380									
1356	1354	1356	1339		1330	1329			1327	1329	
1311	1311	1311								1313	
1280	1275	1277	1260	1269	1258	1258	1283	1282	1285	1281	
1248	1248	1247	1239	1229	1240	1239	1249	1249	1248	1256	
1228	1225	1227					1231	1230	1228	1228	C-N amide or Amide III
1175	1173	1176	1177	1177	1177	1176			1176	1177	
1139	1125	1139									
1111		1114								1112	
1060	1065	1061				1057					

<sup>§</sup> peaks from Schlecht *et al.* (1974)

<sup>†</sup> from Gu and Karthikeyan (2005)

<sup>‡</sup> from the present study

<sup>¶</sup> from Caminati *et al.* (2002)

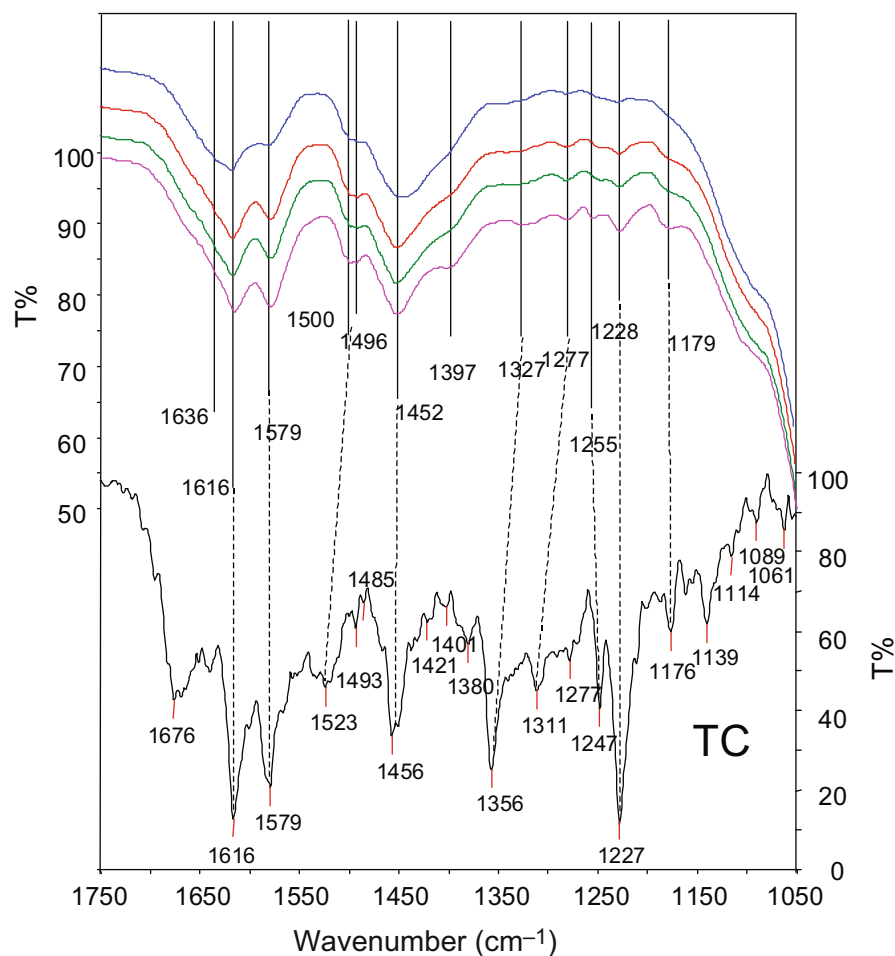


Figure 4. FTIR spectra of SYn-1 intercalated with 0.29, 0.48, 0.52, and 0.54 CEC of TC at equilibrium solution pH values of 5, 4, 3.8, and 3.4 (top to bottom).

#### FTIR of intercalated TC

The bands at 1616 and 1580  $\text{cm}^{-1}$  were assigned to the C=O stretching in tetracycline rings A and C, respectively (Caminati *et al.*, 2002). The location of these bands may be sensitive to the interaction between the rings and the solid substrates. TC complexation with hydroxyapatite resulted in a shift from 1616  $\text{cm}^{-1}$  to 1600  $\text{cm}^{-1}$  (Myers *et al.*, 1983). In contrast, these two bands remained in the same position with respect to bulk TC when TC was mixed with dipalmitoyl phosphatidic acid (DPPA), suggesting that major interactions were absent (Caminati *et al.*, 2002). Moreover, the band at 1616  $\text{cm}^{-1}$  remained in the same location but the band at 1580  $\text{cm}^{-1}$  disappeared after TC complexed with Al or Fe hydrous oxides (Gu and Karthikeyan, 2005).

In the present study, the locations of these two bands remained the same after TC intercalation into SWy-2, SAz-1, and SYn-1 (Tables 1 and 2), suggesting that the uptake of TC by these minerals was not due to complexation and the interaction between the C=O groups in ring A or C and the siloxane surface of the

smectites was minimal. As a short distance is needed for interactions to occur between the functional group and the surface of the basal siloxane surfaces of smectite, the minimal interaction suggests that the distance between the C=O in ring A or C and the smectite surface is not close, indicating that rings A and C may not be parallel to the basal surface of the smectite.

In addition, Myers *et al.* (1983) assigned the band at 1580  $\text{cm}^{-1}$  to keto-enol functional groups on rings B and C and observed a shift to 1560  $\text{cm}^{-1}$  with diminishing intensity after TC complexation with hydroxyapatite. In the present study, the 1580  $\text{cm}^{-1}$  band remained the same for SAz-1, SWy-2, and SYn-1, again confirming that the uptake of TC by these minerals was not due to surface complexation. The peak shifted to 1595–1598  $\text{cm}^{-1}$  after TC intercalated into SHCa-1. As the equilibrium solution pH after TC intercalation into SHCa-1 was high (Li *et al.*, 2010), the shift in this band is more likely to be due to changes in pH.

The bands at 1659 and 1508  $\text{cm}^{-1}$  were assigned to the amide I and amide II bands. They were located at

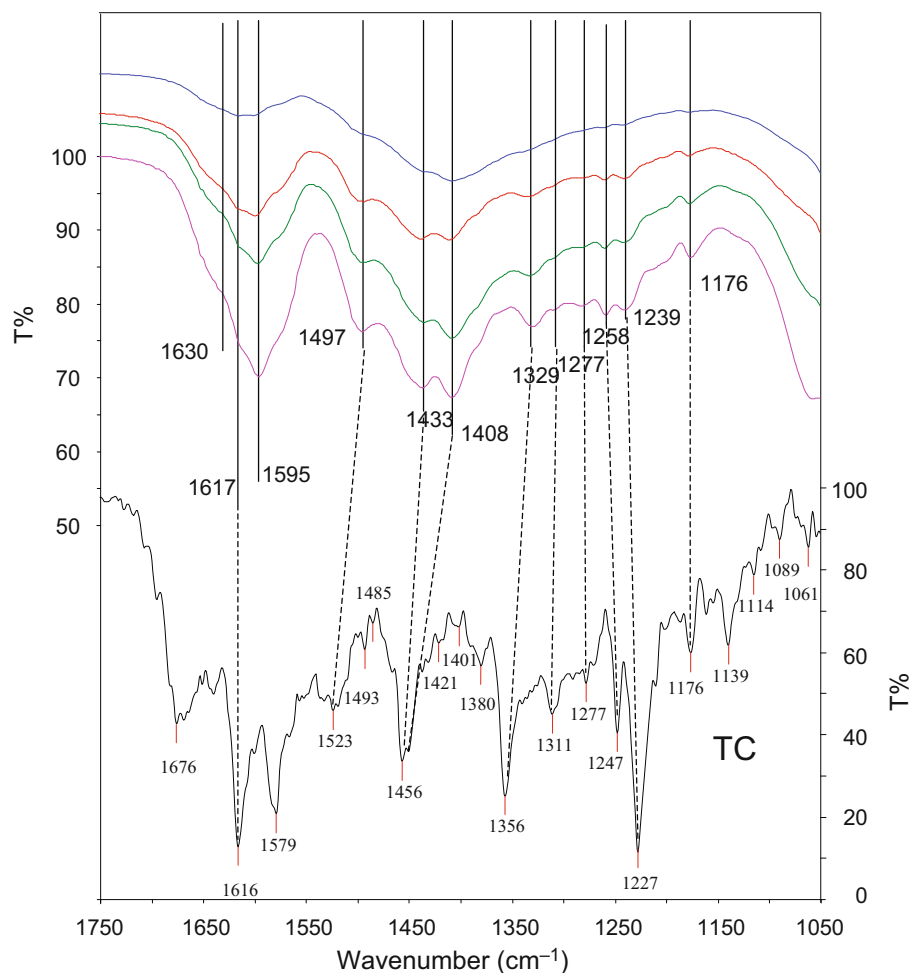


Figure 5. FTIR spectra of SHCa-1 intercalated with 0.34, 0.68, 1.2, and 1.23 CEC of TC at equilibrium solution pH values of 8, 8, 7.3, and 7 (top to bottom).

1665 and  $1530\text{ cm}^{-1}$  in the pure TC, and the amide I band disappeared or shifted to  $1616\text{ cm}^{-1}$  after complexation with hydroxylapatite (Myers *et al.*, 1983). A band shift of  $10\text{--}12\text{ cm}^{-1}$  relative to crystalline TC was attributed to a specific interaction between ring A of TC and the polar head group of DPPA (Caminati *et al.*, 2002). In the present study, the bands of amide I and II for crystalline TC were located at  $1676$  and  $1523\text{ cm}^{-1}$ . The amide I band could not be resolved after TC intercalation into the swelling clays due to the presence of strong OH deformation of water at  $1630\text{ cm}^{-1}$ . In contrast, the amide II band shifted to  $1515\text{ cm}^{-1}$  when TC was intercalated into SWy-2, and further to  $1500\text{ cm}^{-1}$  when TC was intercalated into SAz-1 and SYn-1 (Figures 2–4). The shift of the amide II band compared with the crystalline TC suggested a strong interaction between the amide group and the clay surfaces *via* hydrogen bonding.

The C=C skeleton band at  $1455\text{ cm}^{-1}$  shifted  $\sim 20\text{ cm}^{-1}$  to a lower frequency and was attributed to complexation with hydroxylapatite (Myers *et al.*, 1983).

In contrast, the band at  $1455\text{ cm}^{-1}$  in the present study remained in the same location after TC intercalation into SAz-1, SWy-2, and SYn-1, again suggesting that complexation was not responsible for the uptake of TC by these minerals. However, the  $1455\text{ cm}^{-1}$  peak shifted  $\sim 20\text{ cm}^{-1}$  to a lower frequency after TC intercalation into SHCa-1 at a greater pH, which may suggest that the shift is more likely to be due to changes in pH instead of complexation.

#### *Influence of deuteration on band shift*

The band position corresponding to the OH deformation of water at  $1630\text{ cm}^{-1}$  did not change for any of the smectites, suggesting that complete exchange between D and H in the interlayer water could not be achieved at  $65^\circ\text{C}$  in 7 days (Figure 6). As the interlayer water was associated with interlayer cations, and no cation exchange was associated with the deuteration process, the band position remained the same.

The spectrum of deuterated TC showed significant band shifts and even band disappearance (Figure 6). The amide I

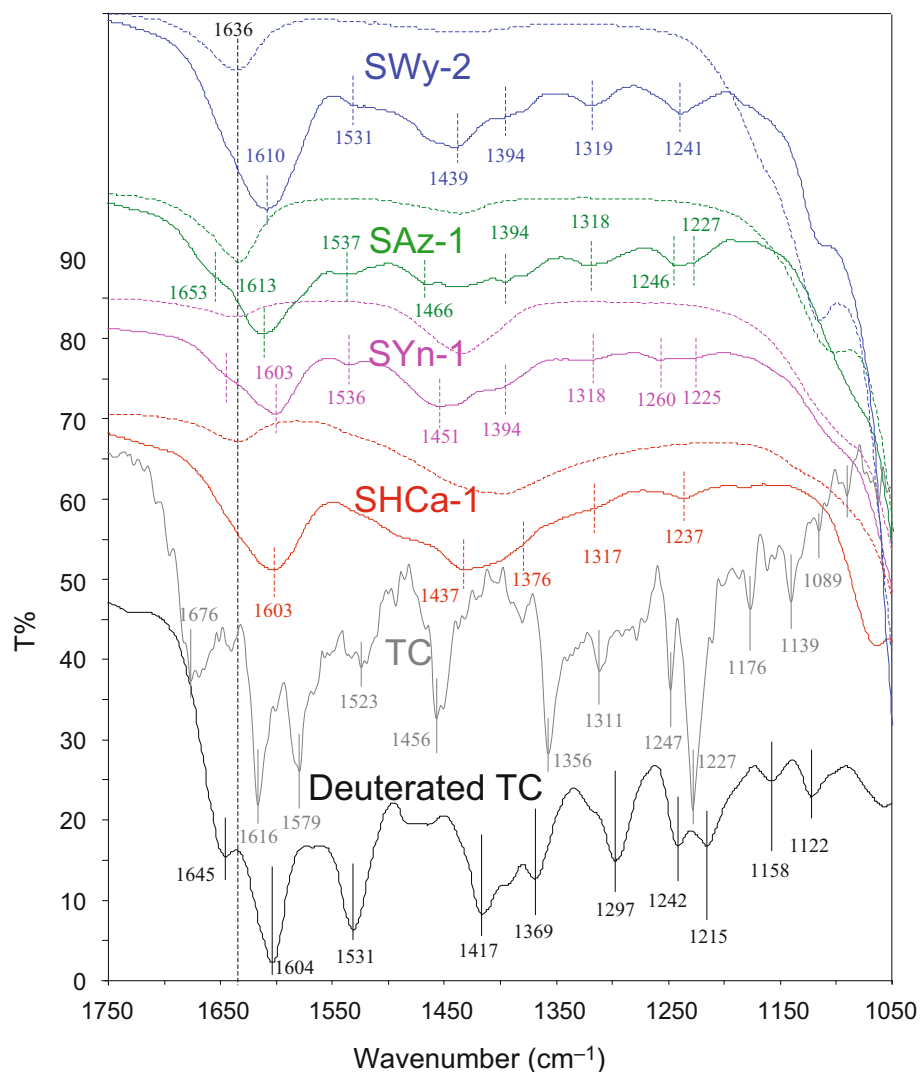


Figure 6. FTIR spectra of deuterated TC adsorbed on smectites (solid lines) and deuterated smectites (dashed lines). Deuterated TC is also shown to compare band positions.

band shifted from 1676 to 1645  $\text{cm}^{-1}$ , the band for C=O of ring A at 1616  $\text{cm}^{-1}$  shifted to 1604  $\text{cm}^{-1}$ , and the band for C=O of ring C at 1579  $\text{cm}^{-1}$  shifted to 1531  $\text{cm}^{-1}$ . These results agree well with those of Dzigielewski *et al.* (1976). The amide II band at 1523  $\text{cm}^{-1}$  disappeared, as expected (Zhang *et al.*, 1992), after D/H exchange in  $\text{D}_2\text{O}$  solution, thus confirming a complete D/H exchange under the given conditions.

Like deuterated TC, the position of the band from the C=O group in ring A shifted from 1616 to 1603 for all TC-intercalated smectites, while that of the band from C=O in ring C shifted from 1580 to 1535 in TC-intercalated SAz-1, SWy-2, and SYn-1 (Figure 6). The band from C=O in ring C is missing from TC-intercalated SHCa-1 at high pH after deuteration, as in the case of non-deuterated TC intercalation in SHCa-1. Similar to the FTIR spectra of deuterated TC, again the amide II of TC band was absent after

deuterated TC intercalation into smectites. The disappearance of this amide II band confirms an absence of hydrogen bonding between amide and the clay surface after D/H exchange.

#### XRD analyses of TC and TC-intercalated swelling clay minerals

The XRD patterns of TC crystallized from solution at pH 4–5 and 8.7 are almost identical (data not shown) and matched that obtained by Thangadurai *et al.* (2005) very well, confirming that the TC used was indeed in its HCl form.

To further elucidate the intercalation of TC into the interlayer space of smectites, samples representing a range of TC loadings into the smectites were analyzed by XRD (Figure 7). For SWy-2 at TC intercalation of 0.40 CEC, the XRD pattern showed a distinct peak plus a shoulder at 12.8 Å. Thereafter a systematic increase in  $d_{001}$  spacing



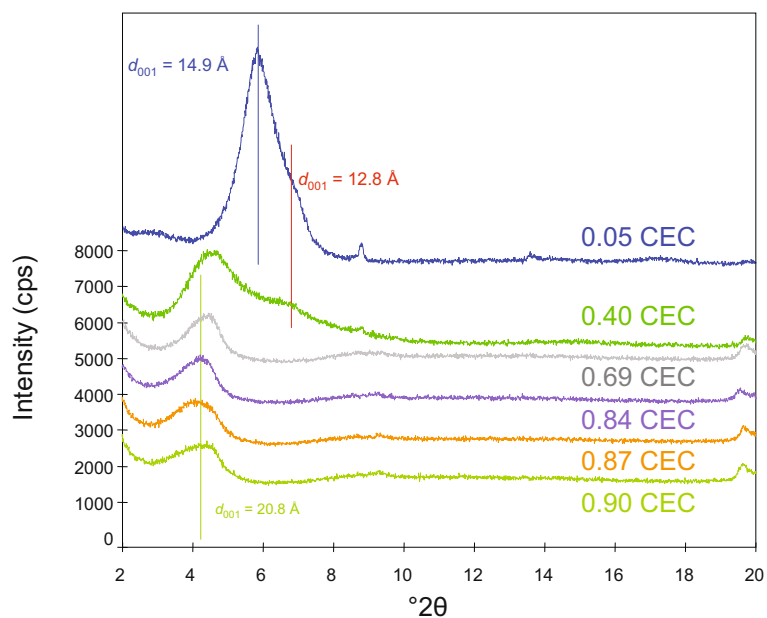


Figure 7. XRD patterns of SWy-2 intercalated with different amounts of TC at pH 6–8.

was found as the amount of TC intercalation increased. At the intercalation level of 0.84 CEC the  $d_{001}$  spacing reached a maximum of 20.8 Å. The  $\text{Na}^+$ -SWy-2 with one layer of water had a  $d$  spacing of 12.5 Å, which could be reduced to 10.0 Å after full dehydration. Thus, the replacement of  $\text{Na}^+$  by TC resulted in a net increase in  $d$  spacing of 8.3 Å compared to  $\text{Na}^+$ -SWy-2, or 10.8 Å compared to a fully collapsed structure.

SAz-1 is a  $\text{Ca}^{2+}$ -montmorillonite with two layers of interlayer water. TC intercalation to levels greater than 0.46 CEC resulted in a  $d_{001}$  spacing expansion to 22.3 Å, or an increase in interlayer distance of 12.3 Å compared to a fully collapsed structure (Figure 8). Similar results were found for TC intercalation into SHCa-1. Raw SHCa-1 had a  $d_{001}$  spacing of 13.0 Å. At a TC intercalation level of 0.50 CEC, the  $d_{001}$  spacing

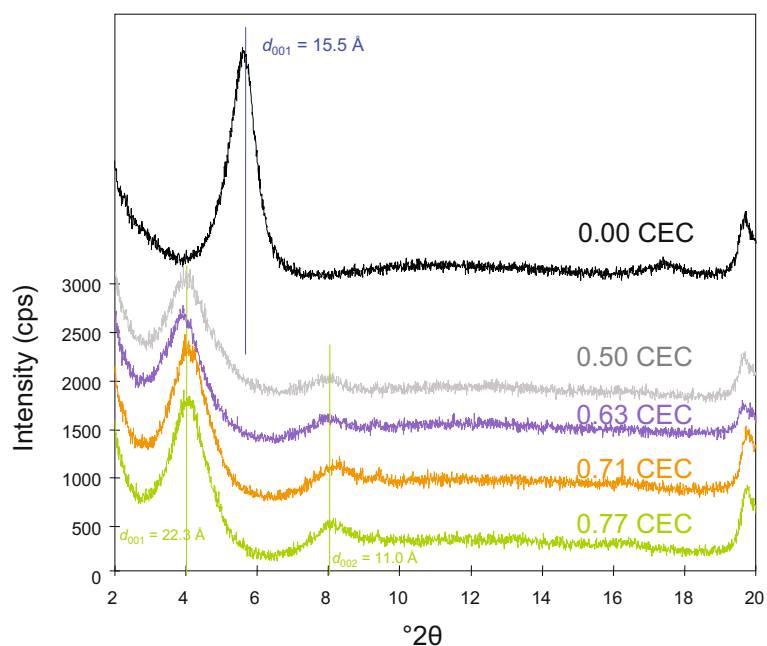


Figure 8. XRD patterns of SAz-1 intercalated with different amounts of TC at pH 4–6.

expanded to 23.6 Å (Figure 9). Significant peak broadening was seen, however, suggesting breakdown of crystallite size along the *c* axis direction.

SYn-1 is a synthetic mica-montmorillonite containing  $\text{NH}_4^+$  in the interlayer (Madejová and Komadel, 2001). Although significant peak broadening could be seen as the level of TC intercalation increased, the  $d_{001}$  spacing remained constant in spite of progressive TC adsorption to a maximum of 0.45 CEC (Figure 10), due to mineral delamination (Lee and Kim, 2002; Ogawa *et al.*, 2003). As such, the adsorption of TC on SYn-1 is believed to occur on the external surfaces instead of intercalated into the interlayer space.

#### Mechanism of TC adsorption by smectites

The most incontrovertible evidence for adsorption of TC into the interlayer space is the expansion of the interlayer in three of the four clays tested. The mechanisms governing intercalation of TC are not agreed upon completely by many researchers, however. The most credited mechanisms for TC uptake by different substrates were cation exchange, surface complexation, hydrophobic interaction, and cation bridging.

Considering that the likelihood of hydrophobic interaction or surface protonation is small, cation exchange is much more likely to be the mechanism for TC uptake by charged minerals, even at greater pH values when the TC molecules are in zwitterionic or mono-anionic forms. For the latter case, the simulta-

neous removal of  $\text{H}^+$  from solution and co-adsorption of  $\text{H}^+$  accompanying TC adsorption make TC retention on smectite minerals possible (Li *et al.*, 2010). Thus, adsorption of  $\text{H}^+$  as the counterion accompanying TC adsorption would be a more plausible explanation for TC adsorption than any of the others proposed, which results in an increase in pH to a neutral or even weakly alkaline state. In addition, the stoichiometric release of metal cations accompanying TC uptake further confirmed that cation exchange was the main mechanism for TC uptake and intercalation into smectites (Li *et al.*, 2010). Thus, the replacement of interlayer cations by protonated TC resulted in interlayer expansion and intercalation.

Complexation was proposed as the predominant mechanism over cation exchange for the zwitterionic form of TC molecules, based on the similarities among the FTIR spectra of TC-intercalated montmorillonites at pH 5.0, 8.7, and 11.0 and that of the TC-Ca complex (Porubcan *et al.*, 1978). Due to the low sensitivity of OTC distribution coefficient in zwitterionic form,  $K_D^{\text{OTC}^0}$ , to ionic strength relative to that in cationic form,  $K_D^{\text{OTC}^+}$ , a previous study (Figueroa *et al.*, 2004) suggested that a surface-complexation mechanism was important for the uptake of the OTC zwitterion species. Others (Gu and Karthikeyan, 2005) indicated that TC complexation with hydrous Al oxide and hydrous Fe oxide could be occurring at the tricarbonylamide (C-1:C-2:C-3 in ring A) and carbonyl (C-11 in ring C) functional groups. However, the FTIR analysis in the present study failed to

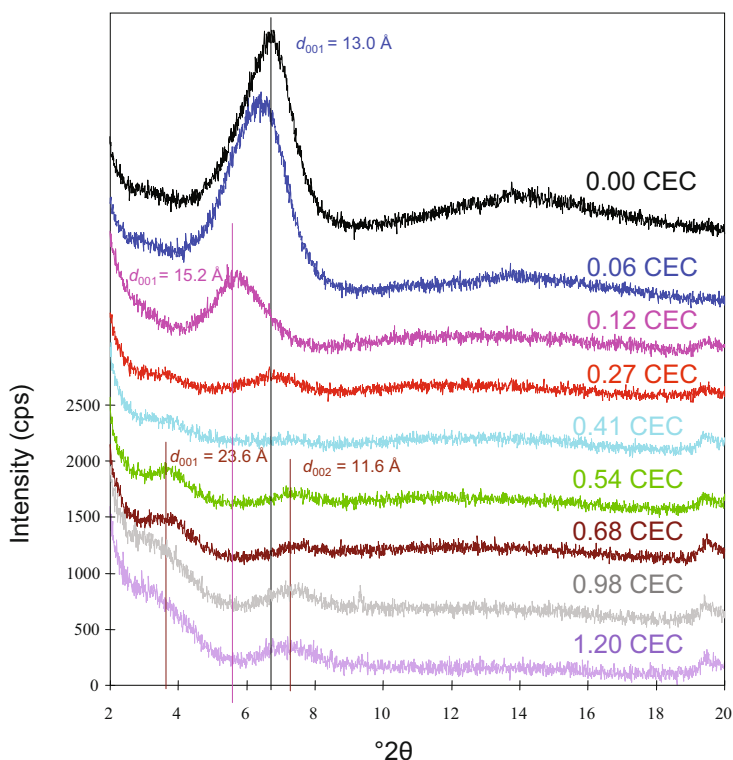


Figure 9. XRD patterns of SHCa-1 intercalated with different amounts of TC at pH 8–9.

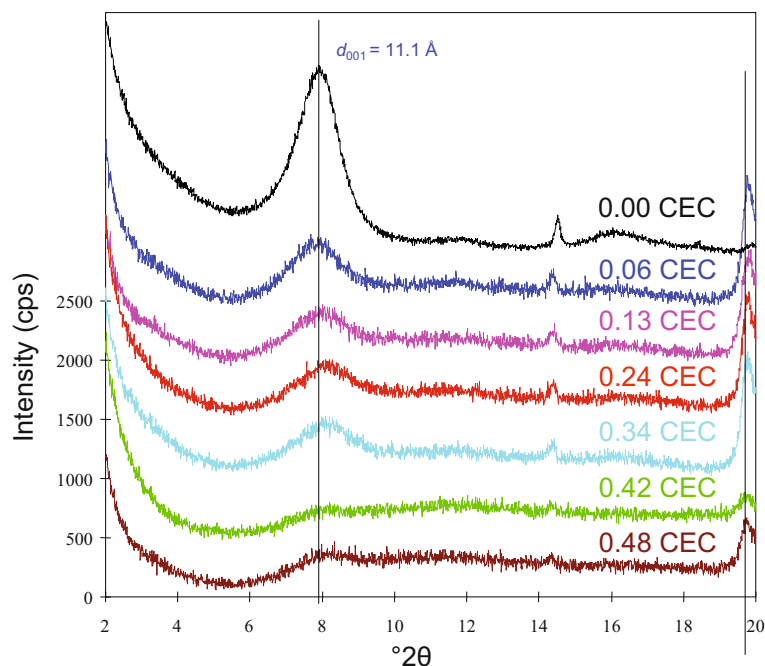


Figure 10. XRD patterns of SYn-1 intercalated with different amounts of TC at pH 4–6.

find strong evidence for surface complexation as the mechanisms for TC intercalation in smectites.

Hydrophobic interaction of the net neutral OTC zwitterion with montmorillonite was also considered as a possible mechanism for TC uptake (Kulshrestha *et al.*, 2004). However, a methanol wash of the clay recovered <5% of OTC mass adsorbed, ruling out physical adsorption by van der Waals interactions as a significant interaction mechanism for OTC (Figueroa *et al.*, 2004).

Surface protonation has been proposed to explain sorption of amino acids and TC from solutions in which zwitterions of these compounds dominate (Porubcan *et al.*, 1978; Browne *et al.*, 1980). For OTC, surface protonation could be considered as  $\text{OTC}^0 + \equiv\text{-H}^+$  (protonated surface)  $\rightarrow \equiv\text{-HOTC}^+$  (Figueroa *et al.*, 2004). The pH of SWy-2 suspension was  $\sim 8$ – $9$ , however. At this high pH range, the surface is unlikely to be protonated compared to that at a low pH. Therefore, surface protonation is unlikely as a major mechanism for TC adsorption on montmorillonite.

#### TC interlayer configuration

Many different interlayer distances have been reported following TC intercalation into montmorillonite. An interlayer distance of 6.8–7.3 Å in good agreement with the smallest dimension of 6.3 Å was reported by Porubcan *et al.* (1978). An interlayer distance of 10.3 Å was observed for OTC intercalation into SWy-2 at pH 1.5 (Kulshrestha *et al.*, 2004) but the TC intercalation level was not provided in that study. The interlayer distance of low-charge SWy-2 at a TC intercalation maximum in the present study was 10.8 Å,

similar to that observed by Kulshrestha *et al.* (2004). For high-charge SAz-1, the interlayer distance increased to 12.3 Å at the TC intercalation maximum.

In contrast to SWy-2 and SAz-1, the interlayer distance did not change in SYn-1 after TC adsorption, suggesting that adsorption was on the outer surfaces instead of intercalation. The significant decrease in peak height of the 001 reflection as the amount of TC adsorption increased confirmed that delamination occurred instead of intercalation due to its smaller layer charge and larger surface area. Finally, for SHCa-1, the interlayer distance was 13.6 Å at pH 8–9, which agrees well with the observation of OTC intercalation in SWy-2 at pH 11 (Kulshrestha *et al.*, 2004). In addition, significant decreases in peak height were also noticed as the amount of TC adsorbed was >0.12 CEC. At 0.41 CEC adsorption, the XRD pattern was essentially flat. As the amount of TC adsorption increased further, however, two extremely low, broad peaks re-appeared. The re-appearance of 001 XRD peaks may suggest that greater amounts of TC intercalation might help to restore somewhat the vertical integrity along the *c* direction.

Tetracycline can exist in different conformations depending on the pH. A twisted conformation occurs in acidic to neutral solutions, in which the dimethylamino group lies above the ring system (Duarte *et al.*, 1999; Othersen *et al.*, 2003), while an extended conformation dominates in basic solutions, in which the dimethylamino group lies below the plane defined by the ring system (Wessels *et al.*, 1998). The totally protonated, twisted conformation of TC is 12.9 Å long, 6.2 Å high,

and 7.5 Å thick (Gambinossi *et al.*, 2004). Based on the fact that the  $d$  spacing expansion is greater than the thickness of TC in this conformation, Porubcan *et al.* (1978) proposed that the TC molecules occupy a tilted

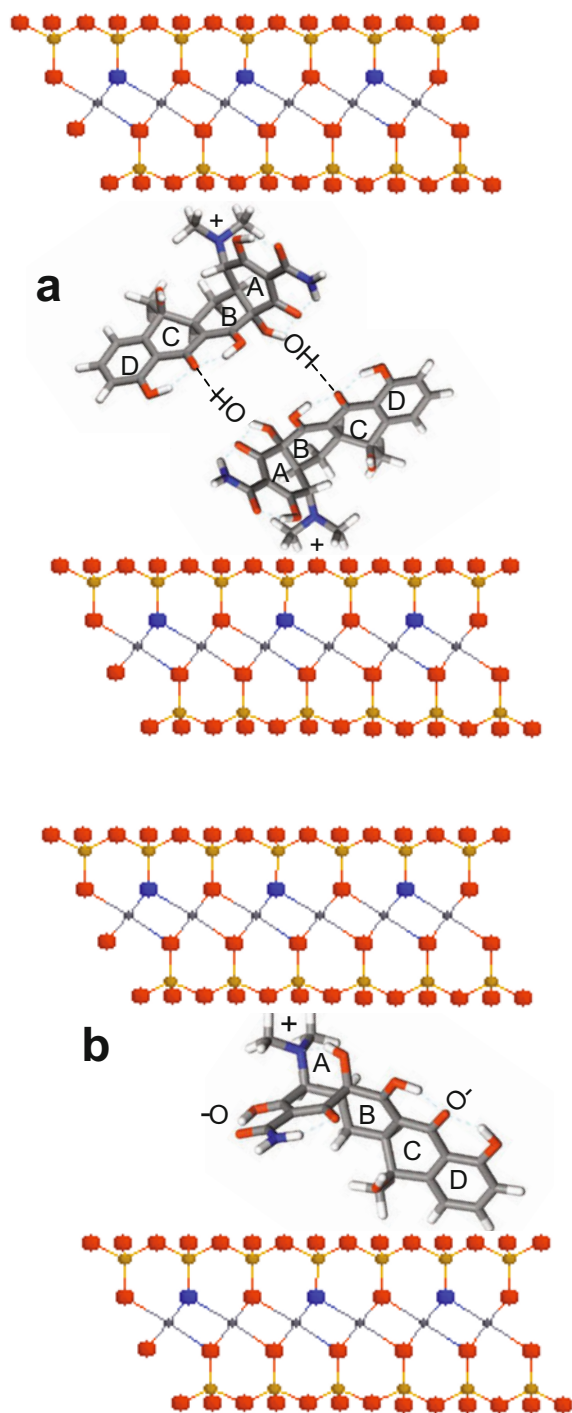


Figure 11. Intercalation of TC with twisted conformation into the interlayer space of montmorillonite tilted at an angle of 45° (a) and with extended conformation (b).

orientation in the interlayer space of montmorillonite. Under this condition, the positive charge of the dimethylammonium group would have a better interaction with the negatively charged surfaces (Figure 11a). In contrast, as the TC molecules adopt the extended conformation at high pH, the intercalated molecules in SHCa-1 could retain this configuration in the interlayer (Figure 11b). The intermolecular arrangement would then depend on how tightly the TC molecules can pack in the interlayer space. Because the amide II vibrational band at 1523  $\text{cm}^{-1}$  is most sensitive to the amount of TC intercalation in smectites, the shift in this band position will indicate the extent to which the extended conformation has occurred among the intercalated TC molecules. As the amount of TC intercalation increases systematically, the band position shifts to a greater wavenumber and closer to that of crystalline TC when intercalated into  $\text{Na}^+$ - and  $\text{Ca}^{2+}$ -montmorillonite (Table 1). The shift to a higher frequency may indicate a transition of intercalated TC molecules from a more loosely to a more closely packed arrangement.

## CONCLUSIONS

Tetracycline (TC) intercalates into the interlayer space of smectites SWy-2, SAz-1, and SHCa-1 but adsorbs only to the external surfaces of SYn-1. The intercalation mechanism is caused by cation exchange rather than by surface complexation, protonation, or hydrophobic adsorption. The intercalated TC molecules adopt a tilted orientation with the dimethylammonium group interacting directly with the negatively charged surfaces of the minerals regardless of whether the TC molecular conformation is in the twisted or extended form. As the amount of TC intercalation increases, a transition apparently occurs in the intercalated TC molecules from a loosely to a close-packed arrangement.

## ACKNOWLEDGMENTS

Funding from National Cheng Kung University (NCKU) for the project of Promoting Academic Excellence and Developing World Class Research Centers to support Prof. Li's short-term stay in NCKU is greatly appreciated.

## REFERENCES

- Al-Rifai, J.H., Gabelish, C.L., and Schäfer, A.I. (2007) Occurrence of pharmaceutically active and non-steroidal estrogenic compounds in three different wastewater recycling schemes in Australia. *Chemosphere*, **69**, 803–815.
- Batt, A.L. and Aga, D.S. (2005) Simultaneous analysis of multiple classes of antibiotics by ion trap LC/MS/MS for assessing surface water and groundwater contamination. *Analytical Chemistry*, **77**, 2940–2947.
- Blackwell, P.A., Kay, P., and Boxall, A.B.A. (2007) The dissipation and transport of veterinary antibiotics in a sandy loam soil. *Chemosphere*, **67**, 292–299.
- Borden, D. and Giese, R.F. (2001) Baseline studies of The Clay Minerals Society source clays: cation exchange capacity measurements by the ammonia-electrode method. *Clays and*

- Clay Minerals*, **49**, 444–445.
- Caminati, G., Focardi, C., Gabrielli, G., Gambinossi, F., Mecheri, B., Nocentini, M., and Puggelli, M. (2002) Spectroscopic investigation of tetracycline interaction with phospholipid Langmuir–Blodgett films. *Materials Science and Engineering C*, **22**, 301–305.
- Carballa, M., Omil, F., Lema, J.M., Llompart, M., Garcia-Jares, C., Rodriguez, I., Gomez, M., and Ternes, T. (2004) Behavior of pharmaceuticals, cosmetics and hormones in a sewage treatment plant. *Water Research*, **38**, 2918–2926.
- Chang, P.-H., Li, Z., Yu, T.-L., Munkhbayer, S., Kuo, T.-H., Hung, Y.-C., Jean, J.-S., and Lin, K.-H. (2009a) Sorptive removal of tetracycline from water by palygorskite. *Journal of Hazardous Materials*, **165**, 148–155.
- Chang, P.-H., Jean, J.-S., Jiang, W.-T., and Li, Z. (2009b) Mechanism of tetracycline sorption on rectorite. *Colloids and Surfaces A: Physicochemical and Engineering Aspects*, **339**, 94–99.
- Dzigiulewski, J., Hanuza, J., and Jezowska-Trzebiatowska, B. (1976) *Bulletin De L'Academie Polnoaise Des Sciences serie des sciences chimiques*, **XXIV** (4), 307–322.
- Dogan, A.U., Dogan, M., Onal, M., Sarikaya, Y., Aburub, A., and Wurster, D.E. (2006) Baseline studies of The Clay Minerals Society Source Clays: specific surface area by the Brunauer Emmett Teller (BET) method. *Clays and Clay Minerals*, **54**, 62–66.
- Duarte, H.A., Carvalho, S., Paniago, E.B., and Simas, A.M. (1999) Importance of Tautomers in the chemical behavior of tetracyclines. *Journal of Pharmaceutical Science*, **88**, 111–120.
- Figueroa, R.A. and Mackay, A.A. (2005) Sorption of oxytetracycline to iron oxides and oxide-rich soils. *Environmental Science & Technology*, **39**, 6664–6671.
- Figueroa, R.A., Leonard, A., and MacKay, A.A. (2004) Modeling tetracycline antibiotic sorption to clays. *Environmental Science & Technology*, **38**, 476–483.
- Gambinossi, F., Mecheri, B., Nocentini, M., Puggelli, M., and Caminati, G. (2004) Effect of the phospholipid head group in antibiotic-phospholipid association at water–air interface. *Biophysical Chemistry*, **110**, 101–117.
- Gu, C. and Karthikeyan, K.G. (2005) Interaction of tetracycline with aluminum and iron hydrous oxides. *Environmental Science & Technology*, **39**, 2660–2667.
- Gu, C., Karthikeyan, K., Sibley, S.D., and Pedersen, J.A. (2007) Complexation of the antibiotic tetracycline with humic acid. *Chemosphere*, **66**, 1494–1501.
- Kim, S., Eichhorn, P., Jensen, J.N., Weber, A.S., and Aga, D.S. (2005) Removal of antibiotics in wastewater: effect of hydraulic and solid retention times on the fate of tetracycline in the activated sludge process. *Environmental Science & Technology*, **39**, 5816–5823.
- Kolpin, D.W., Furlong, E.T., Meyer, M.T., Thurman, E.M., Zaugg, S.D., Barber, L.B., and Burton, H.T. (2002) Pharmaceuticals, hormones, and other organic wastewater contaminants in U.S. streams, 1999–2000: A national reconnaissance. *Environmental Science & Technology*, **36**, 1202–1211.
- Kulshrestha, P., Giese, Jr. R.F., and Aga, D.S. (2004) Investigating the molecular interactions of oxytetracycline in clay and organic matter: Insights on factors affecting its mobility in soil. *Environmental Science & Technology*, **38**, 4097–4105.
- Kümmerer, K. (2009) Antibiotics in the aquatic environment – A review – Part I. *Chemosphere*, **75**, 417–434.
- Lee, S.Y. and Kim, S.J. (2002) Delamination behavior of silicate layers by adsorption of cationic surfactants. *Journal of Colloid and Interface Science*, **248**, 231–238.
- Leypold, C.F., Reiher, M., Brehm, G., Schmitt, M.O., Schneider, S., Matousek, P., and Towrie, M. (2003) Tetracycline and derivatives – assignment of IR and Raman spectra via DFT calculations. *Physical Chemistry Chemical Physics*, **5**, 1149–1157.
- Li, Z., Chang, P.-H., Jean, J.-S., Jiang, W.-T., and Wang, C.-J. (2010) Interaction between tetracycline and smectite in aqueous solution. *Journal of Colloid and Interface Science*, **341**, 311–319.
- Madejová, J. and Komadel, P. (2001) Baseline studies of The Clay Minerals Society source clays: infrared methods. *Clays and Clay Minerals*, **49**, 410–432.
- Mermut, A.R. and Lagaly, G. (2001) Baseline studies of The Clay Minerals Society source clays: layer-charge determination and characteristics of those minerals containing 2:1 layers. *Clays and Clay Minerals*, **49**, 393–397.
- Miao, X.S., Bishay, F., Chen, M., and Metcalfe, C.D. (2004) Occurrence of antimicrobials in the final effluents of wastewater treatment plants in Canada. *Environmental Science & Technology*, **38**, 3533–3541.
- Myers, H.M., Tochon-Danguy, H.J., and Baud, C.A. (1983) IR absorption spectrophotometric analysis of the complex formed by tetracycline and synthetic hydroxyapatite. *Calcified Tissue International*, **35**, 745–749.
- Ogawa, M., Ishii, T., Miyamoto, M., and Kuroda, K. (2003) Intercalation of a cationic azobenzene into montmorillonite. *Applied Clay Science*, **22**, 179–185.
- Othersen, O.G., Beierlein, F., Lanig, H., and Clark, T. (2003) Conformations and tautomers of tetracycline. *Journal of Physical Chemistry B*, **107**, 13743–13749.
- Parolo, M.E., Savini, M.C., Vallés, J.M., Baschini, M.T., and Avena, M.J. (2008) Tetracycline adsorption on montmorillonite: pH and ionic strength effects. *Applied Clay Science*, **40**, 179–186.
- Porubcan, L.S., Serna, C.J., White, J.L., and Hem, S.L. (1978) Mechanism of adsorption of clindamycin and tetracycline by montmorillonite. *Journal of Pharmaceutical Science*, **67**, 1081–1087.
- Sarmah, A.K., Meyer, M.T., and Boxall, A.B.A. (2006) A global perspective in the use, sales, exposure pathways, occurrence, fate and effects of veterinary antibiotics (VAs) in the environment. *Chemosphere*, **65**, 725–759.
- Sassman, S. and Lee, L. (2005) Sorption of three tetracyclines by several soils: Assessing the role of pH and cation exchange. *Environmental Science & Technology*, **39**, 7452–7459.
- Schlecht, K.D., Dix, R.B., and Tamul, M.J. (1974) Internal reflection spectra of several tetracyclines. *Applied Spectroscopy*, **28**, 38–40.
- Thangadurai, S., Abraham, J.T., Srivastava, A.K., Moorthy, M.N., Shukla, S.K., and Anhaneyulu, Y. (2005) X-ray powder diffraction patterns for certain  $\beta$ -lactam, tetracycline and macrolide antibiotic drugs. *Analytical Sciences*, **21**, 833–838.
- Turku, I., Sainio, T., and Paatero, E. (2007) Thermodynamics of tetracycline adsorption on silica. *Environmental Chemistry Letters*, **5**, 225–228.
- Wang, Y.-J., Jia, D.-A., Sun, R.-J., Zhu, H.-W., and Zhou, D.-M. (2008) Adsorption and cosorption of tetracycline and copper(II) on montmorillonite as affected by solution pH. *Environmental Science & Technology*, **42**, 3254–3259.
- Wessels, J.M., Ford, W.E., Szymczak, W., and Schneider, S. (1998) The complexation of tetracycline and anhydrotetracycline with  $Mg^{2+}$  and  $Ca^{2+}$ : A spectroscopic study. *Journal of Physical Chemistry B*, **102**, 9323–9331.
- Zhang, Y., Lewis, R.N.A.H., Hodges, R.S., and McElhaney, R.N. (1992) FTIR spectroscopic studies of the conformation and amide hydrogen exchange of a peptide model of the hydrophobic transmembrane  $\alpha$ -helices of membrane proteins. *Biochemistry*, **31**, 11572–11578.

(Received 22 September 2009; revised 27 May 2010; Ms. 402; A.E. F. Bergaya)